

See discussions, stats, and author profiles for this publication at: <https://www.researchgate.net/publication/6843859>

# Investigating the Dynamic Nature of the Interactions between Nuclear Proteins and Histones upon DNA Damage Using an Immobilized Peptide Chemical Proteomics Approach

ARTICLE *in* JOURNAL OF PROTEOME RESEARCH · OCTOBER 2006

Impact Factor: 4.25 · DOI: 10.1021/pr060278b · Source: PubMed

---

CITATIONS

7

---

READS

24

7 AUTHORS, INCLUDING:



**Eef Dirksen**

Synthon

7 PUBLICATIONS 202 CITATIONS

SEE PROFILE



**Jacqueline Cloos**

VU University Medical Center

160 PUBLICATIONS 2,970 CITATIONS

SEE PROFILE



**Rob M J Liskamp**

University of Glasgow

413 PUBLICATIONS 10,961 CITATIONS

SEE PROFILE



**Albert J R Heck**

Utrecht University

683 PUBLICATIONS 21,637 CITATIONS

SEE PROFILE

## Investigating the Dynamic Nature of the Interactions between Nuclear Proteins and Histones upon DNA Damage Using an Immobilized Peptide Chemical Proteomics Approach

Eef H. C. Dirksen,<sup>†</sup> Martijn W. H. Pinkse,<sup>†</sup> Dirk T. S. Rijkers,<sup>‡</sup> Jacqueline Cloos,<sup>§</sup>  
Rob M. J. Liskamp,<sup>‡</sup> Monique Slijper,<sup>†</sup> and Albert J. R. Heck<sup>\*,†</sup>

*Departments of Biomolecular Mass Spectrometry and Medicinal Chemistry, Utrecht Institute for Pharmaceutical Sciences and Bijvoet Center for Biomolecular Research, Utrecht University, Sorbonnelaan 16, 3584 CA Utrecht, The Netherlands, and Section Tumor Biology, Department of Otolaryngology/Head-Neck Surgery, VU University Medical Center, Amsterdam, The Netherlands*

Received June 9, 2006

As a result of the complexity and dynamic range of the cellular proteome, including mutual interactions and interactions with other molecules, focused proteomic approaches are important to study subsets of physiologically important proteins. In one such approach, a small molecule or part of a protein is immobilized on a solid phase and used as bait to fish out interacting proteins from complex mixtures such as cellular lysates. Here, such a chemical proteomics experiment is presented to explore the range of proteins that interact with the N-terminal tail of core histones. Therefore, a core histone consensus N-terminal tail (NTT) peptide was synthesized and immobilized on agarose. Interactions between histone NTTs and proteins are extremely important as they regulate chromatin structure, which is important in many DNA-related processes, like transcription and DNA repair. Induction of DNA damage, like DNA double strand breaks, is known to trigger chromatin remodeling events through interactions between histone NTTs and so-called histone chaperones. Therefore, we set out to investigate specific changes in interactions of nuclear proteins before and shortly after DNA double strand break induction. Over 700 proteins were found to bind specifically to the NTT peptide, which makes our study the most comprehensive proteomic survey of the broad spectrum of nuclear proteins interacting with the NTT of core histones in nucleosomes. Apart from a few exceptions, the abundance of the majority of NTT binding proteins was found to be unchanged following DNA damage. However, an in-depth analysis of protein phosphorylation (we detected more than 90 unique sites in about 60 proteins) revealed that the phosphorylation status of several proteins involved in chromatin remodeling changes upon DNA damage. We observed that in these differentially phosphorylated chaperones are part of closely interacting protein complexes involved in regulatory mechanisms at the crossroads of nucleosome assembly, DNA replication, transcription, and the early onset of DNA damage repair.

**Keywords:** chemical proteomics • DNA damage • histone chaperones • chromatin remodeling • titanium oxide • phosphorylation

### Introduction

The study of the genome has provided insight into the functioning of cells and the important role of proteins therein. However, understanding protein function within complex cellular networks is needed to enable, for example, the discov-

ery of novel drug targets and their mechanisms of action. Even though the present proteomics methods are able to resolve complex mixtures of proteins, they are often challenged by the dynamic range of the proteome. Therefore, an increasing number of approaches that focus on a subset of proteins within a proteome have been designed, making use of the affinity of a particular subgroup for a certain molecule. This can be done by using a multifunctional substrate-mimicking probe that reacts and binds covalently to proteins/enzymes of interest, enabling selective enrichment of the modified proteins. A reported example is the selective tagging of metalloproteases through coordination of the metal ion in the active site by an hydroxamate-functionalized probe carrying a photoactivatable moiety and a fluorophore to visualize the modified enzymes.<sup>1,2</sup>

\* Correspondence to: Albert J. R. Heck, Department of Biomolecular Mass Spectrometry, Utrecht University, Sorbonnelaan 16, 3584 CA Utrecht, The Netherlands. Fax, (+31) 30 2518219; e-mail, a.j.r.heck@chem.uu.nl.

<sup>†</sup> Department of Biomolecular Mass Spectrometry, Utrecht Institute for Pharmaceutical Sciences and Bijvoet Center for Biomolecular Research, Utrecht University.

<sup>‡</sup> Department of Medicinal Chemistry, Utrecht Institute for Pharmaceutical Sciences and Bijvoet Center for Biomolecular Research, Utrecht University.

<sup>§</sup> Department of Otolaryngology/Head-Neck Surgery, VU University Medical Center.

Even though covalent modification provides the most convenient way of enriching proteins of interest, similar strategies have been applied to other enzyme classes, such as protein kinases, in an approach referred to as affinity proteomics, making use of high-affinity noncovalently binding interactors. To name a few examples, Knockaert et al.<sup>3</sup> investigated the intracellular targets of paullone, a cyclin-dependent kinase and GSK-3 inhibitor, used against cancers and neurodegenerative disorders. Their experiment enriched not only for the expected targets GSK-3  $\alpha$  and  $\beta$ , but also for a completely new interactor, malate dehydrogenase. This shed new light on the possible mechanism(s) of action of this drug. In addition, the coupling of a complete protein, recombinant O<sup>6</sup>-methylguanine-DNA methyltransferase, as a bait to solid support has been shown. Incubation with a complex protein mixture revealed that this methyltransferase not only functions in DNA repair, but also integrates this process with other cellular events, such as replication and cell cycle progression.<sup>4</sup> Furthermore, by using immobilized tyrosine-containing peptides, tyrosine phosphorylation-driven interactions in the EGFR signaling pathway could be elucidated.<sup>5</sup> Next to that, immobilization of DNA sequences allowed the selective purification of transcription factors.<sup>6</sup> These examples reveal that affinity-based approaches may provide very selective methodologies to focus on particular protein–protein and protein–small molecule interactions. Here, we describe a related approach to study in detail nucleosome-related protein–protein interactions.

DNA inside a cell is stored in chromatin in the nucleus. Chromatin, which is a dynamic higher-order structure, is an eloquent example of protein–DNA interactions. The protein part mainly consists of the four core histones (H2A, H2B, H3, and H4) that make up the nucleosomes around which DNA is wrapped in a ‘four pair’ structure (two histone H2A–H2B and two histone H3–H4 pairs,<sup>7</sup> see Figure 1C). Even though it is believed that histone–DNA interactions are rather static, chromatin can adopt markedly different conformations.<sup>8</sup> Most of the time, chromatin is densely packed and stabilized by linker histones and a variety of other factors. This densely packed chromatin structure, that is, heterochromatin, generally inhibits the binding of transcriptional regulators. To enable transcription, chromatin structure has to open up. This change in structure is mediated by interactions between the N-terminal tails of core histones and other proteins, such as acetyl- (HAT) and methyltransferases (HMT). The histone N-terminal tail (NTT) that contains several basic (lysine and arginine) amino acids protrudes from the nucleosome where it can interact both with negatively charged DNA and with proteins involved in DNA-related processes. Upon modification of basic residues in the histone N-terminal tails by HATs and HMTs, the strong interactions between the tails and DNA are disrupted, which opens up chromatin. More recently, it was stated that chromatin density acts as a barrier to the recruitment of DNA repair and DNA damage signaling proteins at sites of DNA damage.<sup>9</sup>

Even though it is known that the histone NTTs provide a binding platform for a large number of proteins, the important mechanisms that regulate these interactions, and thereby coordinate chromatin remodeling events, are largely unknown. To address these issues, we affinity-purified proteins interacting with core histone NTTs from cellular nuclear extracts. By reason of the nature of these interactions, one can choose between two extremities: a very targeted approach in which, for example, a specifically acetylated form of one of the core histones’ NTT is used as bait. Here, on the other hand, we

studied the range of interactions between nuclear proteins and a core histone N-terminal tails in an exploratory fashion using a *consensus* NTT peptide, lacking any post-translational modifications. By using this model peptide that contains conserved amino acid motifs from core histone NTTs (H2A, H2B, H3, and H4, see Figure 1A and 1B), we anticipated to pull down a more comprehensive range of histone NTT-interacting proteins. To investigate the dynamics of interactions, proteins were enriched by affinity pull-downs from nuclear lysates both of control cells and cells in which DNA double strand breaks (DSBs) were induced during 30 min using bleomycin.<sup>10</sup> Over 700 proteins were found to specifically bind to the immobilized peptide before and shortly after DNA damage induction. Next to the possible recruitment of specific proteins, the phosphorylation status of the histone NTT-interacting proteins was analyzed using a twofold strategy to enrich for phosphorylated peptides. This revealed that a number of proteins known to be involved in chromatin remodeling become either phosphorylated or dephosphorylated upon DNA damage induction. The identification of several new DNA damage-induced phosphorylation sites on histone chaperones suggests that DNA-related processes, such as nucleosome assembly, DNA replication, transcription, and repair are integrated.<sup>11</sup>

## Experimental Procedures

**Cell Cultures, DSB Induction, and Preparation of Nuclear Extracts.** Human lymphoblastoid cell culturing, methods for DNA damage induction and the purification of nuclei from human lymphoblastoid cells as well as the subsequent extraction of proteins from nuclei were performed as described before.<sup>12</sup> Briefly, human lymphoblastoid cells were either not challenged or challenged using 10  $\mu$ M bleomycin for 30 min. After harvesting and washing, nuclei were purified using two sequential sucrose washes (2.4 and 1 M, respectively). Nuclei were hypertonically lysed during 1 h at 4 °C, and after centrifugation, the supernatants were used for further study.

**Peptide Immobilization, Enrichment, and in-Solution Digestion of Histone-Binding Proteins.** The core histone N-terminal tail consensus peptide Ac-SGRGKAGKKGRKGAKTRQC-NH<sub>2</sub> was synthesized using Fmoc/tBu solid phase peptide synthesis protocols on a ABI433A peptide synthesizer and subsequently immobilized via its C-terminal cysteine residue as described previously<sup>12</sup> (see Figure 1B). Beads were washed and stored in PBS containing 0.05% sodium azide. One milligram of nuclear protein lysate was buffer-exchanged to IPH-E buffer containing 50 mM Tris·HCl, pH 8, 325 mM NaCl, and 0.5% Triton X-100 and incubated with 25  $\mu$ L of immobilized peptide–agarose slurry. After incubation on a rotating device for 1 h at 4 °C, the supernatant was removed and the beads were washed three times with IPH-E buffer. To find out which proteins bind specifically to the consensus peptide, all lysines in the peptide were acetylated using NHS-acetyl in 200 mM Na<sub>2</sub>CO<sub>3</sub> (pH 8.5) during 1 h at room temperature. As a control, this peptide was also used for an affinity pull-down experiment. Bound proteins were subsequently dissolved in a solution of 8 M urea in 25 mM ammonium bicarbonate, pH 8, and incubated with 750 ng of endoproteinase LysC (Roche Diagnostics) for 4 h at 37 °C. Following reduction and alkylation using 2 mM DTT and 4 mM iodoacetamide, respectively, the sample was diluted to 2 M urea with 50 mM ammonium bicarbonate, pH 8, and incubated overnight with 750 ng of trypsin at 37 °C. In parallel, bound proteins were visualized using standard 1D SDS-PAGE.

**Strong Cation Exchange Chromatography.** Strong cation exchange was performed using two Zorbax BioSCX-Series II columns (i.d., 0.8 mm; l, 50 mm; particle size, 3.5  $\mu\text{m}$ ), a Famos autosampler (LCPackings, Amsterdam, The Netherlands), a Shimadzu LC-9A binary pump, and a SPD-6A UV-detector (Shimadzu, Tokyo, Japan). Prior to SCX chromatography, protein digests were desalted using a small plug of C18 material (3M Empore C18 extraction disk) packed into a GELoader Tip similar to as previously described.<sup>13</sup> The eluate was dried completely by vacuum centrifugation and subsequently reconstituted in 20% acetonitrile, 0.05% formic acid. After injection, the first 10 min were run isocratically at 100% solvent A (0.05% formic acid in 8/2 (v/v) water/acetonitrile, pH 3.0), followed by a linear gradient of 1.3%  $\text{min}^{-1}$  solvent B (500 mM NaCl in 0.05% formic acid in 8/2 (v/v) water/acetonitrile, pH 3.0). A total number of 25 SCX fractions (1 min each, i.e., 50  $\mu\text{L}$  elution volume) were manually collected and dried in a vacuum centrifuge.

**TiO<sub>2</sub> Purification of Phosphorylated Peptides.** The early eluting fractions from the SCX separation were reconstituted in 50% acetonitrile and 5% formic acid and subjected to phosphopeptide purification using TiO<sub>2</sub>.<sup>14</sup> After the sample was loaded onto the TiO<sub>2</sub> microcolumn,<sup>15</sup> the column was washed with 20  $\mu\text{L}$  50% acetonitrile and 5% formic acid. Phosphopeptides were eluted using 10  $\mu\text{L}$  of 1.25% ammonia in water (pH 10.5) and directly mixed with 10  $\mu\text{L}$  of 2% formic acid in water. The flow-through of the TiO<sub>2</sub> microcolumns was completely dried, reconstituted in 0.1 M acetic acid in water, and subjected to nanoLC–MS analysis.

**On-Line Nanoflow Liquid Chromatography FT-ICR–MS.** Dried residues were reconstituted in 10  $\mu\text{L}$  of 0.1 M acetic acid and were analyzed by nanoflow liquid chromatography using an Agilent 1100 HPLC system (Agilent Technologies, Waldbronn, Germany) comprising of a solvent degasser, a binary pump, and a thermostated wellplate autosampler, coupled on-line to a 7-Tesla LTQ-FT mass spectrometer (Thermo Electron, Bremen, Germany). The liquid chromatography part of the system was operated in a setup essentially as described previously.<sup>16</sup> Aqua C18, 5  $\mu\text{m}$ , (Phenomenex, Torrance, CA) resin was used for the trap column, and ReproSil-Pur C18-AQ, 3  $\mu\text{m}$ , (Dr. Maisch GmbH, Ammerbuch, Germany) resin was used for the analytical column. Peptides were trapped at 5  $\mu\text{L}/\text{min}$  in 100% solvent A (0.1 M acetic acid in water) on a 2 cm trap column (100  $\mu\text{m}$  i.d., packed in-house) and eluted to a 25 cm analytical column (50  $\mu\text{m}$  i.d., packed in-house) at  $\sim 150$  nL/min in a 50-min gradient from 0 to 40% solvent B (0.1 M acetic acid in 8/2 (v/v) acetonitrile/water). The eluent was sprayed via emitter tips (made in-house), butt-connected to the analytical column. The mass spectrometer was operated in data-dependent mode, automatically switching between MS and MS/MS and neutral loss driven MS<sup>3</sup> acquisition. Full scan MS spectra (from  $m/z$  300 to 1500) were acquired in the FT-ICR with a resolution of 100 000 at  $m/z$  400 after accumulation to target value of 500 000. The three most intense ions at a threshold above 5000 were selected for collision-induced fragmentation in the linear ion trap at normalized collision energy of 35% after accumulation to a target value of 15 000. The data-dependent neutral loss settings were chosen to trigger a MS<sup>3</sup> event after a neutral loss of either 24.5, 32.6 or  $49 \pm 0.5$   $m/z$  units was detected among the 5 most intense fragment ions.

**Data Analysis.** All MS<sup>2</sup> and MS<sup>3</sup> spectra from each LC–MS run were merged to a single file which was searched using the Mascot search engine (Matrix Science) against the Swiss-Prot

database (version 48.3) with carbamidomethyl cysteine as fixed modification; protein N-acetylation; oxidized methionines; and phosphorylation of serine, threonine, or tyrosine as variable modifications. Trypsin was specified as the proteolytic enzyme, and up to two missed cleavages were allowed. The mass tolerance of the precursor ion was set to 10 ppm, and that of fragment ions was set to 0.5 Da. All phosphorylated peptides identified during Mascot searches were confirmed by manual interpretation of the spectra. Characteristics of all proteins in the set are that have a minimal protein score (Mascot) of 60 and an individual peptide score of 20 (both scores are calculated by the database interface program and are based on the probability of a protein/peptide sequence identification,  $p < 0.05$ ) within an accuracy of 10 ppm. After exclusion of cytoskeletal, ribosomal, and spliceosomal proteins, the analysis set was further focused by applying a semiquantitative ranking based on protein sequence coverage, for which the following criteria were used: at least 1 unique confident peptide identification *per* 100 amino acids in a protein (for proteins smaller than 100 kDa) or at least 5 confident peptide identifications (for proteins larger than 100 kDa) had to be detected. These criteria correct for the fact that larger proteins in general get higher protein scores.

## Results

**Pull-Down of Core Histone N-Terminal Tail Binding Proteins Using Affinity Proteomics.** Numerous proteins that bind to core histone N-terminal tails have been identified, and their specific roles in, for example, nucleosome assembly and/or transcriptional regulation have been characterized (for a review, see ref 17). To gain insight into dynamic chromatin–protein interactions at a more comprehensive scale, the entire subset of proteins interacting with core histone N-terminal tails (NTT) was studied simultaneously using an affinity proteomics approach. Therefore, a peptide was designed that resembled a consensus core histone N-terminal tail sequence (Figure 1A). The peptide is built from the 5 H2A/H4 N-terminal residues (SGRGK), two dibasic (KK and RK) motifs, which occur in H2B and H3, the AK motif from H2A and H4, and finally the RQ motif, as present in the H3 NTT. The peptide was immobilized using the C-terminal cysteine according to the method shown in Figure 1B. We focused on histone-binding proteins within the nuclear proteome because the initial response to DNA damage is expected to occur in the nucleus, and in this way, contamination of nonspecifically binding cytosolic proteins was reduced. All proteins that were affinity-purified from nuclear lysates of human lymphoblastoid cells were analyzed using an in-solution two-step digestion (endoproteinase LysC and trypsin), multidimensional nanoLC and FT (tandem) mass spectrometry.

**Analysis of Proteins That Bind to the Immobilized N-Terminal Tail Peptide.** To get an idea of the composition of the subproteome enriched via the histone N-terminal tail affinity purification, a 1D SDS-PAGE separation of the fractions obtained throughout the enrichment procedure was run, which is shown in Figure 2. From this image we conclude that our affinity purification enriches for quite a few, but specific proteins (see lanes marked E<sub>0</sub> and E<sub>30</sub>), as compared to the flow-through fraction (*marked FT*). In addition, we repeated the pull-down with the immobilized histone NTT peptide of which all lysine residues had been acetylated. After the exact same procedure was used, the fraction eluted from these beads showed nearly no affinity-purified proteins (see lane marked E<sub>0</sub>\* in Figure 2) validating that we are enriching for roughly



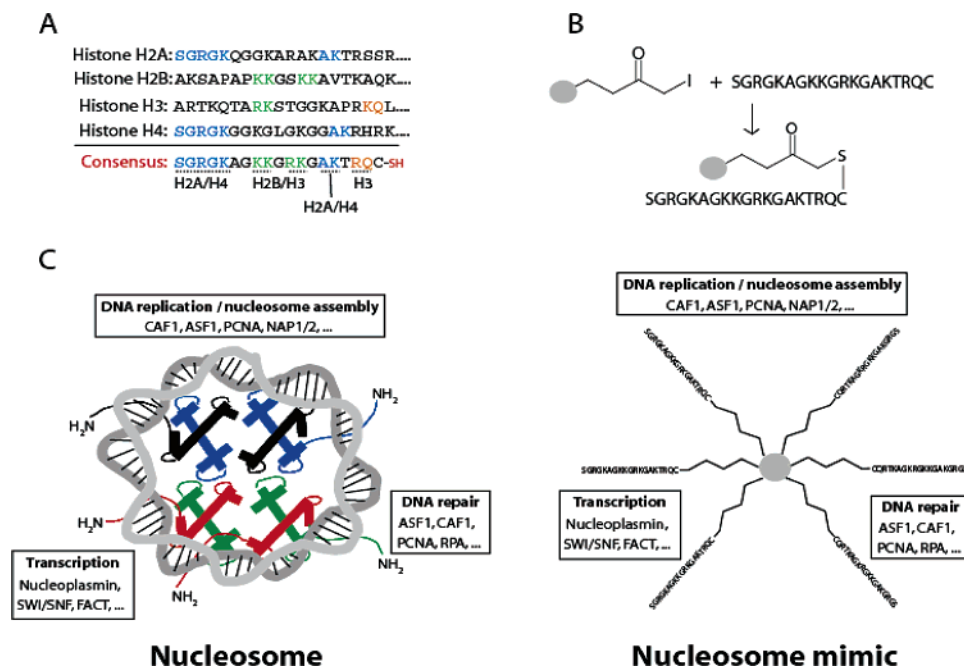


**Figure 1.** (A) Design of the core histone N-terminal consensus peptide used for the affinity pull-downs. It contains various conserved sequence elements from the individual core histone N-terminal tails of H2A, H2B, H3, and H4, as indicated by the colored residues. (B) The peptide was immobilized on iodoacetyl-functionalized agarose beads using the C-terminal cysteine. (C) Schematic overview of core histones in a nucleosome, and examples of histone-interacting proteins involved in nucleosome assembly, transcription, and DNA repair (left panel). The experimental set up (nucleosome mimic) used to enrich for a broad range of histone chaperones using the immobilized core histone consensus sequence is shown in the right panel.

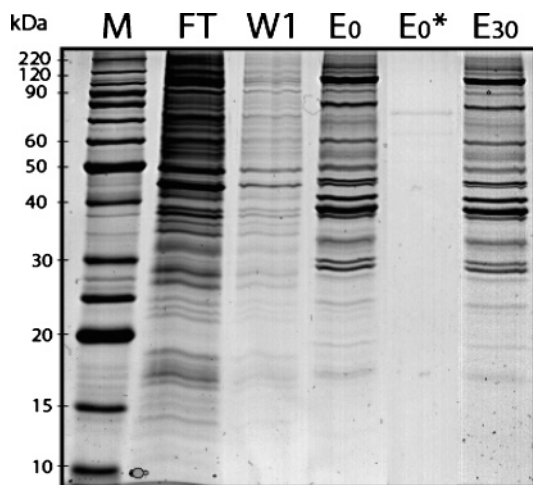


**Figure 2.** 1D SDS-PAGE separation of proteins enriched from a nuclear lysate of human lymphoblastoid cells using the immobilized histone NTT beads (M, molecular weight marker; FT, flow through; W, wash fraction; E0/E30, eluate fractions enriched from control cells and cells in which DNA damage was induced during 30 min). In the lane marked by E0\*, the protein fraction eluted from the beads on which fully lysine-acetylated NTT peptide was immobilized is shown for comparison.

the same, albeit highly specifically binding, proteins in E0 and E30. The complete analysis of the E0 and E30 protein pools binding to the histone NTT was performed in two different ways: first, the eluted fractions were separated using 1D SDS-PAGE, and proteins were identified after in-gel digestion and LC-MS/MS. Even though LC-MS/MS analysis of the in-gel-digested proteins yielded a good overview of the subset of pulled-down proteins (data not shown), a subsequent con-

ducted (gel-free) two-step digestion analysis provided a better coverage of proteins binding to the NTT compared to the 1D-PAGE-MS analysis, especially with respect to high molecular weight proteins. The gel-free approach enabled identification of over 700 (734 and 760 for the  $t = 0'$  and  $t = 30'$  samples, respectively) (compared to 541 and 530, respectively in the gel-based analysis) proteins binding to the immobilized peptide. Protein sets of the GeLC-MS and the gel-free approach largely overlapped. All identifications from the gel-free analysis are given in Supplementary Table 1 of Supporting Information. To further focus on proteins of interest, we implemented a semiquantitative ranking, as described in Experimental Procedures, which was based on the requirement for a protein to be identified by at least one unique peptide *per* 100 amino acids ( $\approx 10$  kDa). Cytoskeletal, ribosomal, and spliceosomal proteins covered approximately 40% of the proteins enriched. Even though some of these proteins have been reported to associate with chromosomes,<sup>18</sup> they will be excluded from the following discussion, as we were primarily interested in proteins more directly involved in chromatin remodeling. An overview of the composition of the final analysis set is given in Figure 3. The qualitative differential binding of proteins to the histone NTT peptide was evaluated by comparing the set of binding proteins enriched from a nuclear lysate of control cells to that of a nuclear lysate of cells in which DNA DSBs were induced. The subset enriched from the cells in which DNA DSBs were induced consisted of 264 proteins, while 260 proteins were detected in the sample enriched from the control cells. The two datasets shared 220 proteins; so 44 proteins were uniquely detected after DNA DSB induction, whereas 40 were only detected before DNA damage induction. An overview of the protein scores for the proteins identified in both runs is given in Figure 4. The plot shows that the majority of proteins is

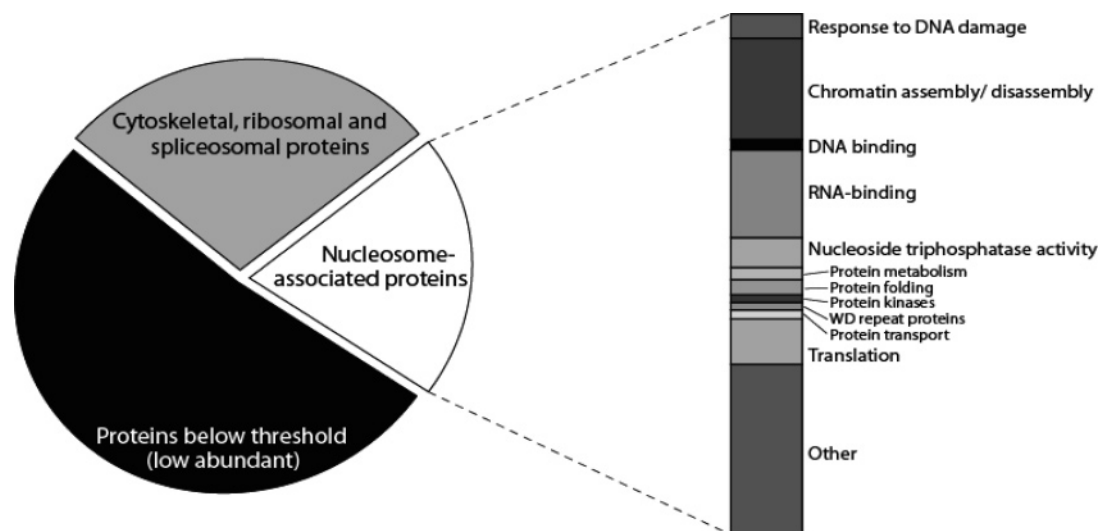


**Figure 3.** Classification of the subset of proteins discussed in the text that was obtained after the semiquantitative ranking and subsequent exclusion of cytoskeletal, ribosomal, and spliceosomal proteins, as described in Experimental Procedures.

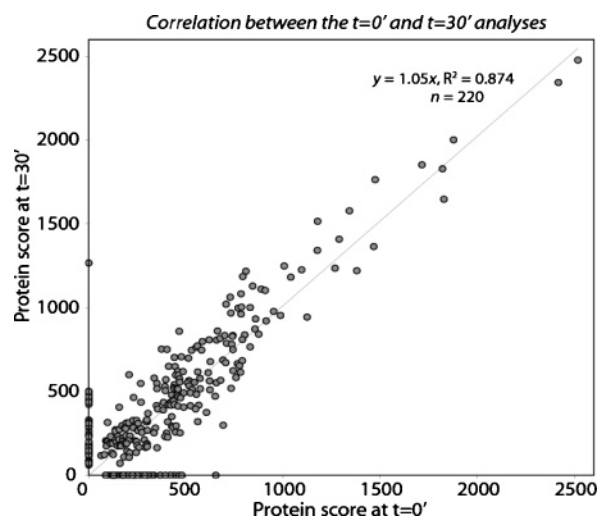


**Figure 4.** Comparative proteome analysis of control cells ( $t = 0'$ ) and cells in which DNA DSBs were induced using bleomycin during 30 min ( $t = 30'$ ). The plot of the scores of all proteins identified in the  $t = 0'$  sample versus the  $t = 30'$  sample reveals that some proteins are only found at one of the timepoints (represented by the dots that lie on the x- and y-axis, respectively). A majority of the proteins however are found in both sets (for examples see Table 1) and can therefore be used to assess the reproducibility. The fact that the protein scores correlate well illustrates the good reproducibility of the two individual analyses.

found in both samples with the same score ( $y = 1.05x$ ,  $R^2 = 0.87$ , see Figure 4), illustrating that the two individual analyses are highly similar and reproducible. The protein score was used as a semiquantitative indication of protein abundance, although we realize that this is only an assumption. Many known histone-/nucleosome-interacting proteins were found to be enriched, exemplified by the list of identified proteins given in Table 1, including all three subunits of a histone deacetylase complex (SAP18, HDAC1, and SIN3a) that enhances transcriptional repression, histone acetyltransferase type B catalytic subunit and subunit 2, nucleosome assembly proteins, and chromatin assembly factor 1. Proteins that were apparently more abundant before DNA damage induction include Mx2-interacting protein, ubiquitin-protein ligase EDD1, and the

**Table 1.** Examples of Proteins That Were Identified after Enrichment from Nuclear Lysates of Human Lymphoblastoid Cells Using the Immobilized Histone N-Terminal Tail Peptide<sup>a</sup>

identified proteins
(Q9UKV3) Apoptotic chromatin condensation inducer in the nucleus
(P39687) Acidic leucine-rich nuclear phosphoprotein 32 A
(P21127) PITSLRE serine/threonine-protein kinase CDC2L1
(O14646) Chromodomain-helicase-DNA-binding protein 1
(O14929) Histone acetyltransferase type B catalytic subunit
(O00422) Histone deacetylase complex subunit SAP18
(Q13547) Histone deacetylase 1
(Q96ST3) Paired amphipathic helix protein Sin3a
(P12956) ATP-dependent DNA helicase II, 70 kDa subunit
(P13010) ATP-dependent DNA helicase II, 80 kDa subunit
(P55209) Nucleosome assembly protein 1-like 1
(O75607) Nucleoplasmin-3
(P78527) DNA-dependent protein kinase catalytic subunit
(Q9NS91) Postreplication repair protein RAD18
(Q09028) Chromatin assembly factor 1 subunit C
(O60264) SWI/SNF related matrix associated actin dependent regulator of chromatin

<sup>a</sup> The code in parentheses is the Swiss-Prot/TrEMBL accession number, followed by the corresponding protein name. The full set of identified proteins is given in Supplementary Table 1 (Supporting Information).

ATP-dependent RNA helicase DDX3X. The PITSLRE serine/threonine protein kinase CDC2L2, Matrin-3, and hnRNP H<sup>1</sup> were only identified after DNA damage induction. However, to date, none of these proteins have been linked to specific DNA damage-related processes.

**Post-Translational Modification of Histone Chaperones upon DNA DSB Induction.** As chromatin remodeling in the onset of the DNA damage response has to occur fast and transcription and translation are time-consuming processes, other activation mechanisms may regulate protein activity in the early response to DNA DSBs. Protein phosphorylation has been described as an activation mechanism for proteins in large numbers of pathways, including DNA repair.<sup>19</sup> Therefore, we studied the role of protein phosphorylation in remodeling events in the early response to DNA damage. Phosphorylated peptides were enriched through SCX at low pH<sup>20</sup> followed by TiO<sub>2</sub> chromatography.<sup>14</sup> The use of a phosphorylation-specific mass spectrometric method<sup>20</sup> further aided the analysis of

Table 2. Phosphopeptides Uniquely Identified Prior to, and after DNA Damage Induction<sup>a</sup>

Phosphopeptides Uniquely Identified in the Untreated Cells (t = 0')			
protein ID	score	peptide	consensus site prediction
Mass (Da)			
1640.63948	57	NUCL_HUMAN (P19338) Nucleolin K.GFGFVDFNS <sup>618</sup> EEDAK.E	S <sup>618</sup> : CK1/CK2
1767.67366	39	YBOX1_HUMAN (P67809) Nuclease sensitive element binding protein 1 R.NYQQNYQNS <sup>165</sup> ESGEK.N	S <sup>165</sup> : CK2
2306.17447	44	NPM_HUMAN (P06748) Nucleophosmin (NPM) K.MSVQPTVS <sup>88</sup> LGGFEITPPVVL.R	S <sup>88</sup> : No pred.
3044.21350	52	-.MEDS <sup>4</sup> MDMDMSPLRPQNYLFGCELK.A + M <sub>OX</sub> , N-t <sub>Ac</sub>	S <sup>4</sup> : CK2, PLK1
3028.21860	45	-.MEDSMDMDMS <sup>10</sup> PLRPQNYLFGCELK.A + N-t <sub>Ac</sub>	S <sup>10</sup> : p38MAPK
1939.78360	56	NP1L4_HUMAN (Q99733) Nucleosome assembly protein 1-like 4 (NAP2) M.ADHS <sup>4</sup> FSDGVPDSVEAAK.N + N-t <sub>Ac</sub>	S <sup>4</sup> : No pred.
Phosphopeptides Uniquely Identified in Cells in Which DNA DSBs Were Induced Using Bleomycin (t = 30')			
2928.07050	64	SSRP_HUMAN (Q08945) Structure-specific recognition protein 1 K.EGMNPSYDEYADS <sup>444</sup> DEQHDAYLER.M	S <sup>444</sup> : CK2
1566.61984	106	CHD1_HUMAN (O14646) Chromodomain-helicase-DNA-binding protein 1 R.RYS <sup>1096</sup> GSDSDSISEGK.R	S <sup>1096</sup> : PKG, GSK3
1646.58617	22	R.RYS <sup>1096</sup> GS <sup>1098</sup> DSDSISEGK.R	S <sup>1098</sup> : No pred.
1549.16	MA	R.RYSGSDSDSISEGK.R	
1092.59433	23	SAFB1_HUMAN (Q15424) Scaffold attachment factor B K.SKGVVIS <sup>576</sup> VK.T	S <sup>576</sup> : CK1

<sup>a</sup> Entries marked with 'MA' reflect identifications that were manually annotated from MS/MS/MS spectra. Since not all of the identified phosphorylation sites are known, a kinase prediction was performed using the NetPhosK algorithm (<http://www.cbs.dtu.dk/services/NetPhosK/>). No pred indicates that NetPhos gave no prediction for a particular phosphorylation site. CK1/2 = casein kinase 1/2, PLK1 = Polo-like kinase, p38MAPK = p38 mitogen-activated protein kinase, PKG = cGMP dependent protein kinase, GSK3 = Glycogen synthase kinase-3.

phosphorylated peptides. More than 100 phosphopeptides were found in the lysates of cells prior to, and 30 min after, DNA damage induction, covering about 90 unique sites from 60 proteins (see Supplementary Table 2, Supporting Information). The majority of the phosphorylated peptides is found in both nuclear extracts indicating that these sites are not significantly regulated in response to DNA DSB induction. More interesting, several unique (uniquely identified by mass spectrometry after DNA damage induction) phosphopeptides were identified that may provide insight into the regulatory mechanisms of particular histone chaperones in the onset of the DNA damage response. A summary of unique phosphopeptides is given in Table 2. As not all of phosphorylation sites given in Table 2 have been described before, a kinase consensus site prediction was performed to find possible kinase(s) for these sites, which are given in Table 2.

An example of DNA damage-induced phosphorylation identified here is shown in Figure 5. This figure illustrates the relative change of a phosphorylated peptide from the structure-specific recognition protein 1 (SSRP1) compared to a coeluting peptide of the Treacle protein (TCOF1) that did not change in abundance upon DNA DSB induction and may therefore be used as an internal standard. The fragmentation spectrum revealed that SSRP1 was phosphorylated on serine-444. This serine lies within a consensus sequence for casein kinase 2 (CK2, DpSD) embedded in the aspartate/glutamate-rich acidic domain of the protein. In addition to serine-444 of SSRP1, two phosphorylation sites on CHD1 in a single tryptic peptide (serine-1096 and 1098), as well as serine-576 of scaffold attachment factor B1 (SAFB1), were found to be phosphorylated upon DNA DSB induction. Apparent DSB-induced phosphatase activity was detected as well; sites in the abundant nuclear phosphoproteins nucleolin and nucleophosmin, in addition to

the acetylated N-terminal part of nucleosome assembly protein 1-like 4 (NAP-2), were dephosphorylated upon DNA DSB induction.

Discussion

**Pull-Down of Core Histone N-Terminal Tail Binding Proteins Using Affinity Proteomics.** Our study represents the first proteomic survey of the broad spectrum of interactions between proteins from a human nuclear lysate and the N-terminal tails (NTT) of core histones in nucleosomes. As can be seen both in Table 1 and Supplementary Table 1 (Supporting Information), many proteins that are known to interact with core histones were enriched through this approach thereby validating the setup of our model system. Generally, domains in proteins that bind to histones within chromatin contain stretches of acidic amino acids (aspartic and glutamic acid) and those are present in many of the identified proteins. We also observed proteins that were most likely enriched via indirect association with the histone NTT peptide, since they are part of functional protein complexes of which only one constituent is known to interact with histone NTTs. This is illustrated by the identification of Ku80 that lacks an acidic histone-binding domain and was probably enriched indirectly through a physical interaction with Ku70. The dimer with Ku70, which contains two aspartate/glutamate-rich regions, is involved in the recognition of DNA lesions.<sup>21</sup>

As illustrated by the 1D-PAGE image (shown in Figure 2) and the more comprehensive gel-free analysis, few qualitative differences were found in the protein sets enriched from control cells and cells in which DNA DSBs were induced. It is unlikely that these differences are a result of changes in protein expression within the time frame of the experiment (30 min), since transcription and translation are believed to take longer

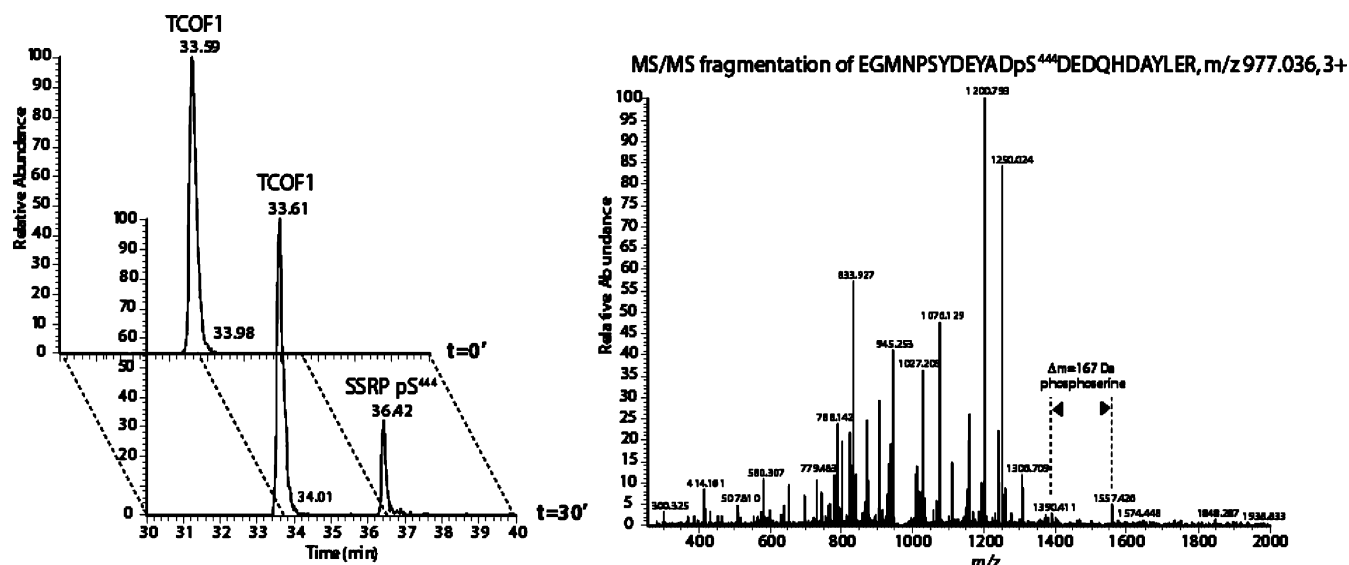


**Figure 5.** Mass spectrometric identification of a phosphorylation site uniquely found upon DNA damage induction. In the left panel, the extracted ion chromatograms of the phosphorylated peptide from structure specific recognition protein 1 (SSRP1) together with that of a peptide originating from the Treacle protein (TCOF1) are given for both data sets. The abundance of the latter peptide did not change upon DNA damage induction and was therefore used as relative internal standard. This illustrates the regulation of the SSRP1 phosphorylation upon DNA damage induction ( $t = 30'$ ). On the right, the MS/MS fragmentation spectrum of the phosphorylated peptide EGMNPSYDEYADpS<sup>44</sup>DEDQHDAYLER is given that revealed serine-444 to be the site of phosphorylation.

in higher eukaryotes. Therefore we expected that proteins uniquely identified either before or after DNA damage induction shuttle from, or are recruited to, the nucleus upon DNA damage induction. The marginal, though possibly interesting, contribution of shuttling to chromatin remodeling processes is not further discussed here.

**Several Proteins Involved in Chromatin Remodeling Are Phosphorylated upon DNA Damage Induction.** To enable a fast cellular response, the subset of proteins that bind to core histone Nucleosome Targeting (NTTs) on nucleosomes can be post-translationally modified, for example, phosphorylated, in the early onset of the DNA damage response. Several of these DNA damage-induced phosphorylation and dephosphorylation events were found in this study, among others on the structure-specific recognition protein 1 on serine-444 (see Figure 5). The role of this identified phosphorylation site on SSRP1, which lies within a consensus sequence for casein kinase 2 (CK2, DpSD), is still unknown. Interestingly, other CK2-phosphorylation sites on SSRP1 have been related to the response to UV-induced DNA damage, resulting in phosphorylation of serine-510, -675, and -688.<sup>22,23</sup> The latter sites were stated *not* to be phosphorylated upon irradiation with  $\gamma$ -radiation, suggesting different regulatory mechanisms upon induction of different types of DNA damage (base oxidation and double strand DNA breaks resulting from UV- and  $\gamma$ -radiation, respectively). This is in line with our results, as these phosphorylation sites were indeed not detected here, which suggests that serine-444 phosphorylation is specific for the response to DNA DSBs.

In addition, two phosphorylation sites on the chromo-domain-helicase-DNA-binding protein 1 (CHD1) were uniquely identified upon DNA DSB induction. Systematic mass spectrometric analysis, using MS<sup>2</sup> and MS<sup>3</sup>, revealed that serine-1096 and serine-1098 within the same tryptic peptide, were the sites of phosphorylation. The peptide was found both singly and doubly phosphorylated. Only a few reports about the effect of phosphorylation on the functioning of CHD1 exist in the literature; therefore, the potentially interesting role of phos-

phorylation on two sites upon DSB induction remains to be established. Scaffold attachment factor B1 (SAFB1) was found to become phosphorylated upon DNA damage induction on serine residue 576. This protein is responsible for the formation of a transcriptome complex by binding to S/MAR (scaffold/matrix attachment region) DNA.

The identified phosphorylation site lies within the part of the protein that both contains the nuclear localization signal and interacts with RNA polymerase II, indicating that this modification either regulates the cellular localization and/or the interaction with RNA polymerase II, thereby possibly repressing transcription in response to DNA damage induction. It is known that phosphorylation can greatly influence the activity of proteins and/or is a trigger for (the disruption of) specific protein-protein interactions. A previously reported example of such activation is the recruitment of phosphorylated chromatin assembly factor 1 (CAF1) to chromatin after UV irradiation of human cells, thereby linking chromatin assembly and DNA repair.<sup>24</sup>

**DNA Damage-Induced Phosphatase Activity Detected on Histone-Interacting Proteins.** In addition to the DNA-damage-induced increase in phosphorylation, DNA damage-specific declines in phosphorylation were also detected: a number of phosphorylated peptides were only found in their phosphorylated forms in the lysates of control cells. An example of such a peptide is the acetylated N-terminal tryptic peptide (phosphorylated on serine-4) from NAP-2 that was found to be dephosphorylated upon DNA damage induction. Phosphorylation of this protein throughout the cell cycle was studied,<sup>25</sup> and this showed that dephosphorylation of NAP-2 triggers its transport into the nucleus. This however did not influence the binding of NAP-2 to histones, as was also found in this study. The protein was shown to be part of several multiprotein complexes together with, for example, histone H1 and CK2 or with DNA topoisomerase I,<sup>26</sup> suggesting that it is involved in several processes other than nucleosome assembly. NAP-2 is



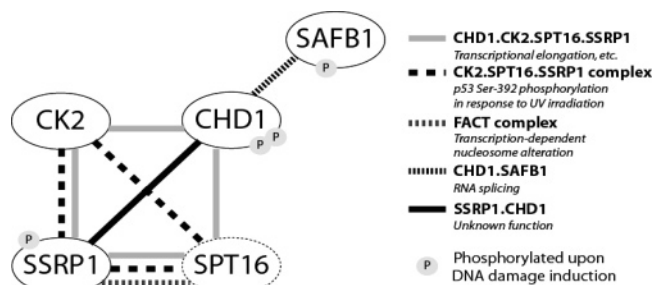


**Figure 6.** Schematic representation of the interplay between histone chaperones that were differentially phosphorylated upon DNA damage induction. Several of the histone-binding proteins identified here are known to be part of several protein complexes that act at several levels of chromatin remodeling and in various pathways, thereby coordinating DNA-related processes. This enables the integration of transcription, RNA splicing, and DNA repair. Lines between proteins indicate that these are part of the same protein complex, and different types of lines resemble different protein complexes. CK2, *casein kinase 2*; CHD1, *chromodomain-helicase-DNA-binding protein 1*; SSRP1, *structure-specific recognition protein 1*; SAFB1, *scaffold attachment factor B1*, SPT16 (resembled by a circle with a dotted line because this protein was not found in our study), *human ortholog of yeast suppressor of Ty insertion mutations*.

phosphorylated by CK2, but the phosphatase responsible for the dephosphorylation of this protein is not known.

**Histone Chaperones Take Part in Multiple Remodeling Complexes Enabling Interplay between DNA-Related Processes.** In the affinity purification described here, primary interactions are expected to take place between stretches of acidic amino acids that are found in proteins and the basic amino acids present in the immobilized NTT peptide. This largely explains the binding of, for instance, SSRP1, SAFB1, NAP-2, and the  $\beta$ -subunit of CK2.

Other subunits of CK2 identified here,  $\alpha$  and  $\alpha'$ , are probably enriched indirectly (while they are bound to subunit  $\beta$ ). CK2 has not only been described to associate with nucleosomes during transcription,<sup>27</sup> but has also been reported to be involved in the DNA damage response by phosphorylating Mdm2.<sup>28</sup>

In our study, SSRP1 was found to be phosphorylated upon DNA damage induction on a serine that lies within a CK2 consensus sequence. SSRP1 has been reported to be a constituent of a multiprotein complex as is illustrated in Figure 6, containing CK2 that specifically phosphorylates serine-392 of p53 in response to DNA damage.<sup>29,30</sup> Moreover, as can be seen in Figure 6, SSRP1 has been described to be part of another complex, named FACT (facilitates chromatin transcription), that is involved in transcriptional regulation.<sup>31</sup> This implicates a link between transcription and DNA repair via chromatin remodeling activities and is concomitant with previous reports on the involvement of histone chaperones in a variety of processes involving DNA, especially transcriptional regulation, and DNA repair.<sup>32–34</sup>

The enrichment of CHD1 through interaction with the NTT peptide is unexpected, since this protein does not contain acidic stretches. It does contain two chromodomains, which have been described to recognize methylated residues in histone NTTs.<sup>35</sup> The fact that CHD1 was detected in both pull-down experiments indicates that the interaction is not influenced by the phosphorylation of serines 1096 and 1098. Nevertheless, this modification might recruit other proteins to

this large histone chaperone and/or possibly triggers the formation of multiprotein complexes. The protein has not been related to the DNA damage response, but it is clear that in transcriptional regulation CHD1 is preferentially located at active, decompacted regions in chromatin,<sup>36</sup> which suggests that this protein helps to maintain chromatin in an open state. This is, of course, also highly favorable for the efficiency of DNA repair. Intriguingly, SSRP1 and SAFB1 have been described to interact with CHD1 (see Figure 6), and it is tempting to assume that these interactions are regulated by phosphorylation of CHD1. The interaction of CHD1 with SSRP1 occurs via an N-terminal segment of CHD1 that lies outside its chromo-domain, but its exact function remains unknown.<sup>37</sup> Yeast two-hybrid experiments conducted to reveal RNA polymerase II elongation factors yielded an interaction between CK2, SSRP1, hSPT16, and CHD1.<sup>38</sup> Finally, the interplay between SAFB1 and CHD1 was described to affect RNA splicing.<sup>39</sup>

## Conclusions

Taken together, the results of our affinity proteomics approach show that most histone chaperones involved in chromatin remodeling are constitutively present in the nucleus both prior as well as after DNA damage induction. When remodeling is required, for example, to allow DNA replication or transcription, specific histone chaperones are recruited to chromatin, which is triggered by post-translational modifications, such as phosphorylation. This was also shown for chaperones in the response to DNA damage: phosphorylation sites on SSRP1, CHD1, and SAFB1 were specifically found upon induction of DNA DSBs. These proteins have previously been described to be part of several protein complexes involved in multiple DNA-related processes of which an overview is given in Figure 6. Additionally, dephosphorylated sites were identified in histone chaperones, such as the nuclear phosphoproteins nucleolin and nucleophosmin as well as in NAP-2. The exact function of these modifications remains to be elucidated. We postulate that these post-translational modifications fulfill a role in the response to DNA DSBs at the level of chromatin remodeling preceding DNA repair, for example, by disrupting or inducing protein–protein interactions on the core histone N-terminal tail platform.

Our approach provides an overview of histone N-terminal tail interacting proteins. Even though we find our approach to be highly sensitive in enrichment, it compromises specificity induced by specific histone sequences and/or post-translational modifications. Our data provides new insights into events that occur immediately upon DNA DSB induction featuring protein networks at the crossroads of nucleosome assembly, DNA replication, transcription, and repair.

**Acknowledgment.** This work was supported by The Netherlands Proteomics Centre.

**Supporting Information Available:** Supplementary Table 1: overview of all proteins identified in the analysis run of the sample enriched from the lysate of control cells ( $t = 0'$ ), and that of cells in which DNA damage was induced for 30 min ( $t = 30'$ ). 'Access' = accession number of the protein in the Swiss-Prot database; 'Mw' = theoretical molecular weight of the protein; 'Score' = Mascot score of the protein; 'Pept' = number of peptides used for identification of the protein; 'Protein name' = protein name(s) and identifier from the Swiss-Prot database. Supplementary Table 2: Overview of phospho-

rylated peptides identified from nuclear lysates of control cells ( $t = 0'$ ), and that of cells in which DNA damage was induced for 30 min ( $t = 30'$ ). Phosphopeptides were identified both from MS/MS and MS/MS/MS fragmentation spectra. 'Observed' = peptide mass observed in the MS spectrum; 'Mr(expt)' = expected molecular weight based on peptide charge; 'Mr(calc)' = theoretical peptide mass; 'Delta' = difference between expected and calculated peptide mass; 'Score' = peptide score from Mascot; 'Expect' = expectance value assigned by Mascot; 'Peptide' = peptide sequence including the previous and next amino acid, to determine cleavage site. Proteins are represented as *protein\_ID*, (*accession number*) *protein name* based on the Swiss-Prot database.

## References

- Chan, E. W.; Chattopadhyaya, S.; Panicker, R. C.; Huang, X.; Yao, S. Q. Developing photoactive affinity probes for proteomic profiling: hydroxamate-based probes for metalloproteases. *J. Am. Chem. Soc.* **2004**, *126*, 14435–14446.
- Saghatelian, A.; Jessani, N.; Joseph, A.; Humphrey, M.; Cravatt, B. F. Activity-based probes for the proteomic profiling of metalloproteases. *Proc. Natl. Acad. Sci. U.S.A.* **2004**, *101*, 10000–10005.
- Knockaert, M.; Wieking, K.; Schmitt, S.; Leost, M.; Grant, K. M.; Mottram, J. C.; Kunick, C.; Meijer, L. Intracellular targets of paullones. Identification following affinity purification on immobilized inhibitor. *J. Biol. Chem.* **2002**, *277*, 25493–25501.
- Niture, S. K.; Doneanu, C. E.; Velu, C. S.; Bailey, N. I.; Srivenugopal, K. S. Proteomic analysis of human O(6)-methylguanine-DNA methyltransferase by affinity chromatography and tandem mass spectrometry. *Biochem. Biophys. Res. Commun.* **2005**, *337*, 1176–1184.
- Schulze, W. X.; Mann, M. A novel proteomic screen for peptide–protein interactions. *J. Biol. Chem.* **2004**, *279*, 10756–10764.
- Yaneva, M.; Tempst, P. Affinity capture of specific DNA-binding proteins for mass spectrometric identification. *Anal. Chem.* **2003**, *75*, 6437–6448.
- Luger, K.; Mader, A. W.; Richmond, R. K.; Sargent, D. F.; Richmond, T. J. Crystal structure of the nucleosome core particle at 2.8 Å resolution. *Nature* **1997**, *389*, 251–260.
- Morales, V.; Giamarchi, C.; Chailleux, C.; Moro, F.; Marsaud, V.; Le Ricousse, S.; Richard-Foy, H. Chromatin structure and dynamics: functional implications. *Biochimie* **2001**, *83*, 1029–1039.
- Wuebbles, R. D.; Jones, P. L. DNA repair in a chromatin environment. *Cell. Mol. Life Sci.* **2004**, *61*, 2148–2153.
- Adema, A. D.; Cloos, J.; Verheijen, R. H.; Braakhuis, B. J.; Bryant, P. E. Comparison of bleomycin and radiation in the G2 assay of chromatid breaks. *Int. J. Radiat. Biol.* **2003**, *79*, 655–661.
- Chakravarthy, S.; Park, Y. J.; Chodaparambil, J.; Edayathumangalam, R. S.; Luger, K. Structure and dynamic properties of nucleosome core particles. *FEBS Lett.* **2005**, *579*, 895–898.
- Dirksen, E. H.; Cloos, J.; Braakhuis, B. J.; Brakenhoff, R. H.; Heck, A. J.; Slijper, M. Human lymphoblastoid proteome analysis reveals a role for the inhibitor of acetyltransferases complex in DNA double-strand break response. *Cancer Res.* **2006**, *66*, 1473–1480.
- Gobom, J.; Nordhoff, E.; Mirgorodskaya, E.; Ekman, R.; Roepstorff, P. Sample purification and preparation technique based on nano-scale reversed-phase columns for the sensitive analysis of complex peptide mixtures by matrix-assisted laser desorption/ionization mass spectrometry. *J. Mass Spectrom.* **1999**, *34*, 105–116.
- Pinkse, M. W.; Uitto, P. M.; Hilhorst, M. J.; Ooms, B.; Heck, A. J. Selective isolation at the femtomole level of phosphopeptides from proteolytic digests using 2D-NanoLC-ESI-MS/MS and titanium oxide precolumns. *Anal. Chem.* **2004**, *76*, 3935–3943.
- Larsen, M. R.; Thingholm, T. E.; Jensen, O. N.; Roepstorff, P.; Jorgensen, T. J. Highly selective enrichment of phosphorylated peptides from peptide mixtures using titanium dioxide microcolumns. *Mol. Cell. Proteomics* **2005**, *4*, 873–886.
- Meiring, H. D.; van der Heeft, E.; ten Hove, G. J.; de Jong, A. P. J. M. Nanoscale LC-MS<sup>2</sup>; technical design and applications to peptide and protein analysis. *J. Sep. Sci.* **2002**, *25*, 557–568.
- Loyola, A.; Almouzni, G. Histone chaperones, a supporting role in the limelight. *Biochim. Biophys. Acta* **2004**, *1677*, 3–11.
- Uchiyama, S.; Kobayashi, S.; Takata, H.; Ishihara, T.; Hori, N.; Higashi, T.; Hayashihara, K.; Sone, T.; Higo, D.; Nirasawa, T.; Takao, T.; Matsunaga, S.; Fukui, K. Proteome analysis of human metaphase chromosomes. *J. Biol. Chem.* **2005**, *280*, 16994–17004.
- Wang, H.; Guan, J.; Perrault, A. R.; Wang, Y.; Iliakis, G. Replication protein A2 phosphorylation after DNA damage by the coordinated action of ataxia telangiectasia-mutated and DNA-dependent protein kinase. *Cancer Res.* **2001**, *61*, 8554–8563.
- Beausoleil, S. A.; Jedrychowski, M.; Schwartz, D.; Elias, J. E.; Villen, J.; Li, J.; Cohn, M. A.; Cantley, L. C.; Gygi, S. P. Large-scale characterization of HeLa cell nuclear phosphoproteins. *Proc. Natl. Acad. Sci. U.S.A.* **2004**, *101*, 12130–12135.
- Jackson, S. P. Sensing and repairing DNA double-strand breaks. *Carcinogenesis* **2002**, *23*, 687–696.
- Li, Y.; Keller, D. M.; Scott, J. D.; Lu, H. CK2 phosphorylates SSRP1 and inhibits its DNA-binding activity. *J. Biol. Chem.* **2005**, *280*, 11869–11875.
- Krohn, N. M.; Stemmer, C.; Fojan, P.; Grimm, R.; Grasser, K. D. Protein kinase CK2 phosphorylates the high mobility group domain protein SSRP1, inducing the recognition of UV-damaged DNA. *J. Biol. Chem.* **2003**, *278*, 12710–12715.
- Martini, E.; Roche, D. M.; Marheineke, K.; Verreault, A.; Almouzni, G. Recruitment of phosphorylated chromatin assembly factor 1 to chromatin after UV irradiation of human cells. *J. Cell Biol.* **1998**, *143*, 563–575.
- Rodriguez, P.; Pelletier, J.; Price, G. B.; Zannis-Hadjopoulos, M. NAP-2: histone chaperone function and phosphorylation state through the cell cycle. *J. Mol. Biol.* **2000**, *298*, 225–238.
- Rodriguez, P.; Ruiz, M. T.; Price, G. B.; Zannis-Hadjopoulos, M. NAP-2 is part of multi-protein complexes in HeLa cells. *J. Cell. Biochem.* **2004**, *93*, 398–408.
- Guo, C.; Davis, A. T.; Yu, S.; Tawfic, S.; Ahmed, K. Role of protein kinase CK2 in phosphorylation nucleosomal proteins in relation to transcriptional activity. *Mol. Cell. Biochem.* **1999**, *191*, 135–142.
- Allende-Vega, N.; Dias, S.; Milne, D.; Meek, D. Phosphorylation of the acidic domain of Mdm2 by protein kinase CK2. *Mol. Cell. Biochem.* **2005**, *274*, 85–90.
- Keller, D. M.; Zeng, X.; Wang, Y.; Zhang, Q. H.; Kapoor, M.; Shu, H.; Goodman, R.; Lozano, G.; Zhao, Y.; Lu, H. A DNA damage-induced p53 serine 392 kinase complex contains CK2, hSpt16, and SSRP1. *Mol. Cell* **2001**, *7*, 283–292.
- Keller, D. M.; Lu, H. p53 serine 392 phosphorylation increases after UV through induction of the assembly of the CK2.hSPT16.SSRP1 complex. *J. Biol. Chem.* **2002**, *277*, 50206–50213.
- Belotserkovskaya, R.; Oh, S.; Bondarenko, V. A.; Orphanides, G.; Studitsky, V. M.; Reinberg, D. FACT facilitates transcription-dependent nucleosome alteration. *Science* **2003**, *301*, 1090–1093.
- Gontijo, A. M.; Green, C. M.; Almouzni, G. Repairing DNA damage in chromatin. *Biochimie* **2003**, *85*, 1133–1147.
- Frit, P.; Kwon, K.; Coin, F.; Aurio, J.; Dubaele, S.; Salles, B.; Egly, J. M. Transcriptional activators stimulate DNA repair. *Mol. Cell* **2002**, *10*, 1391–1401.
- Verger, A.; Crossley, M. Chromatin modifiers in transcription and DNA repair. *Cell. Mol. Life Sci.* **2004**, *61*, 2154–2162.
- Flanagan, J. F.; Mi, L. Z.; Chruszcz, M.; Cymborowski, M.; Clines, K. L.; Kim, Y.; Minor, W.; Rastinejad, F.; Khorasanizadeh, S. Double chromodomains cooperate to recognize the methylated histone H3 tail. *Nature* **2005**, *438*, 1181–1185.
- Lusser, A.; Urwin, D. L.; Kadonaga, J. T. Distinct activities of CHD1 and ACF in ATP-dependent chromatin assembly. *Nat. Struct. Mol. Biol.* **2005**, *12*, 160–166.
- Kelley, D. E.; Stokes, D. G.; Perry, R. P. CHD1 interacts with SSRP1 and depends on both its chromodomain and its ATPase/helicase-like domain for proper association with chromatin. *Chromosoma* **1999**, *108*, 10–25.
- Krogan, N. J.; Kim, M.; Ahn, S. H.; Zhong, G.; Kobor, M. S.; Cagney, G.; Emili, A.; Shilatifard, A.; Buratowski, S.; Greenblatt, J. F. RNA polymerase II elongation factors of *Saccharomyces cerevisiae*: a targeted proteomics approach. *Mol. Cell. Biol.* **2002**, *22*, 6979–6992.
- Tai, H. H.; Geisterfer, M.; Bell, J. C.; Moniwa, M.; Davie, J. R.; Boucher, L.; McBurney, M. W. CHD1 associates with NCoR and histone deacetylase as well as with RNA splicing proteins. *Biochem. Biophys. Res. Commun.* **2003**, *308*, 170–176.

PR060278B